



HAL
open science

Crystal structure and formation of TlPd_3 and its new hydride TlPd_3H

Nadine Kurtzemann, Holger Kohlmann

► **To cite this version:**

Nadine Kurtzemann, Holger Kohlmann. Crystal structure and formation of TlPd_3 and its new hydride TlPd_3H . *Journal of Inorganic and General Chemistry / Zeitschrift für anorganische und allgemeine Chemie*, 2010, 10.1002/zaac.201000012 . hal-00599848

HAL Id: hal-00599848

<https://hal.science/hal-00599848>

Submitted on 11 Jun 2011

HAL is a multi-disciplinary open access archive for the deposit and dissemination of scientific research documents, whether they are published or not. The documents may come from teaching and research institutions in France or abroad, or from public or private research centers.

L'archive ouverte pluridisciplinaire **HAL**, est destinée au dépôt et à la diffusion de documents scientifiques de niveau recherche, publiés ou non, émanant des établissements d'enseignement et de recherche français ou étrangers, des laboratoires publics ou privés.



Crystal structure and formation of TIPd3 and its new hydride TIPd3H

Journal:	<i>Zeitschrift für Anorganische und Allgemeine Chemie</i>
Manuscript ID:	zaac.201000012.R1
Wiley - Manuscript type:	Article
Date Submitted by the Author:	05-Feb-2010
Complete List of Authors:	Kurtzemann, Nadine; Universität des Saarlandes, FR 8.1 Anorganische Festkörperchemie Kohlmann, Holger; Universität des Saarlandes, FR 8.1 Anorganische Festkörperchemie
Keywords:	hydrides, intermetallic phases, in situ, DSC, neutron powder diffraction



ARTICLE

DOI: 10.1002/zaac.200((will be filled in by the editorial staff))

Crystal structure and formation of TlPd_3 and its new hydride TlPd_3H

Nadine Kurtzemann*, Holger Kohlmann

*Dedicated to Prof. Dr. Rüdiger Kniep on the occasion of his 65th birthday.***Keywords:** hydrides; intermetallic phases; in situ; neutron powder diffraction; DSC

TlPd_3 was synthesized from the elements in evacuated silica tubes at 600°C. Alternatively, TlPd_3 was yielded by reduction of the TlPd_3O_4 in N_2 gas atmosphere. Reduction of the oxide in H_2 gas atmosphere resulted in the formation of the new hydride TlPd_3H . The structure of tetragonal TlPd_3 (ZrAl_3 type, space group $I4/mmm$, $a = 410.659(9)$ pm, $c = 1530.28(4)$ pm) was reinvestigated by X-ray and also by neutron powder diffraction as well as the structure of its previously unknown hydride TlPd_3H (cubic anti-perovskite type structure, space group $Pm\bar{3}m$, $a = 406.313(1)$ pm).

In situ DSC measurements of TlPd_3 in hydrogen gas atmosphere showed a broad exothermic signal over a wide temperature range with two maxima at 280°C and at 370°C resulting in TlPd_3H as product. A dependency of lattice parameter of the intermetallic phase on reaction conditions is observed and discussed. Results of hydrogenation experiments at room temperature with gas pressure up to 280 bar hydrogen and at elevated temperatures with very low hydrogen gas pressures (1-2 bar) as well as results of dehydrogenation of the hydrides under vacuum will be discussed.



Universität des Saarlandes, Fachrichtung 8.1. – Anorganische Festkörperchemie, Am Markt Zeile 3, 66125 Dudweiler, Germany
Fax: +49 681 302 70667
E-mail: n.kurtzemann@mx.uni-saarland.de

1. Introduction

Hydrogen absorption and desorption characteristic of intermetallic compounds and also of noble metals as palladium have been scrutinised with regard to electronic and magnetic properties, hydrogen embrittlement, order-disorder transitions etc. in the past [1-12]. Thereby some of palladium rich compounds with Cu-type superstructures containing e. g. Mn [8, 13-20], Mg [21-24], Al [22, 25, 31], Ga [22, 26-28, 31], In [27, 29-31], Tl [27, 32-34] or Sn [35] have been explored. Few of the MPd₃ compounds showed very similar structural changes during hydrogenation forming hydrides MPd₃H_x (M = Mn, Mg or In, x < 1) with a metallic sublattice in the AuCu₃-type structure. These intermetallic compounds crystallize in one of the following superstructures of the Cu-type: AuCu₃, TiAl₃ or ZrAl₃. Our group proposed a gliding mechanism [23] to explain the observed structural changes from the starting structure to the metallic sublattice in the hydride during hydrogen uptake: Comparing configuration and number of octahedral voids in the AuCu₃-type structure of MPd₃ sublattice with those in the other above mentioned structure types an increase of the voids surrounded by six palladium atoms at the expense of those surrounded by five Pd and one M or four Pd and two M is realized. Theoretical calculations for MgPd₃ show that the preference of hydrogen to occupy octahedral sites with only palladium as nearest neighbour is justified by energetic reasons [24]. Gliding along ½ [110] of the domains of antiphases in the TiAl₃- and ZrAl₃-types generates the structure of the AuCu₃ type which offers more only by palladium atoms encircled octahedral sites to incorporate hydrogen atoms as the larger superstructures [23]. To better understand the relation between the mechanism of the hydride formation and the above mentioned gliding operation along ½ [110] it is needful to continue the exploration of hydrogenation behaviour of other palladium rich systems MPd₃ (respectively M_{1-m} M' _m Pd₃) with Cu-type superstructures, e.g. M and M' = Tl, Pb, Sn, In.

TlPd₃ was reported for the first time by Stadelmaier et al. in 1961 to crystallize in the SrPd₃ structure type, a tetragonal distorted variant of the AuCu₃ structure (space group *P* 4/*mmm*, a = 412 pm and c = 381 pm) [32], and later on by Schubert and Bhan et al. [33, 34] who determined the crystal structure as ZrAl₃-type at room temperature and as TiAl₃-type at elevated temperatures. TlPd₃ has not yet been examined in respect of its hydrogenation characteristics, till this day. In this work the crystal structure of TlPd₃ is examined again by X-ray and neutron powder diffraction, results of hydrogenation and dehydrogenation of TlPd₃ are presented and discussed as well as the structure of the new hydride TlPd₃H.

2. Experimental Section

2.1. Synthesis

TlPd₃ powder samples were synthesized from the elements. Palladium (powder <60 μm, 99.9+%, ChemPur or powder, -60 μm, 99.9% ABCR) and thallium (rod, 99.999%, Alfa Aesar) cut in pieces inside an argon filled glove box were heated in evacuated sealed silica tubes at 600°C and typically reground one or more times. The overall reaction time was between 40 and 300 hours. Alternatively the grey intermetallic phase was obtained by decomposition of TlPd₃O₄ at 730°C in nitrogen atmosphere [36, 37], usually within 12 hours. To gain the cardinal red oxide TlPd₃O₄ [36, 37] we embarked a solid state synthesis route not afore known for this oxide: Appropriate amounts of the elements palladium and thallium were prepared as mentioned above and heated at 600°C in air in silica or corundum crucibles for 24 hours with a regrinding step after 12 hours. The oxide was obtained as main phase with less than 3% of TlPd₃ as byproduct. With a heating time of only 12 hours in air or 6 hours even in pure oxygen mixed phases of TlPd₃O₄, Tl₂O₃, TlPd₃ (ZrAl₃-type), PdO and Pd were yielded (which is below called 5-phase-mixture).

The hydride formation was explored either by hydrogenation of the intermetallic phase or by reduction of oxide TlPd₃O₄ or of 5-phase-mixture directly in hydrogen atmosphere (Praxair, 99.999%) in a chamber furnace (Linn HighTherm HT 1400 Vac) with a gas flow rate of 100 ml / min. For both reactions, conditions were typically 12 hours held at 730°C and 1bar hydrogen pressure. The heating rate was 100°C / h or 300°C / h, the cooling rate 200°C / h or 300°C / h. Few hydrogenation experiments were performed within in an autoclave described elsewhere [31] up to 280 bar hydrogen pressure and a maximum temperature of 250°C.

2.2. X-Ray powder diffraction

Powder X-Ray diffraction (XRPD) patterns were recorded on a Huber image plate Guinier diffractometer G670 using CuK_{α1} radiation (λ = 154.053 pm). The measurements were performed using flat transmission samples with the powders fixed on an adhesive tape. Step width of the data was 0.005° in 2θ and silicon was used as internal standard. For Rietveld refinements the programme Full Prof [38] was applied using pseudo-Voigt functions to generate the line shape of the diffraction peaks.

2.3. Neutron powder diffraction and Rietveld refinement

Neutron powder diffraction data (NPD) were collected on the high flux powder diffractometer D20 (Institut Laue Langevin, Grenoble, France) in the range $7^\circ \leq 2\theta \leq 154^\circ$ (step size $\Delta 2\theta = 0.1^\circ$) [39]. The determination of the wavelength $\lambda = 186.893(2)$ pm was performed by measuring a silicon standard in a vanadium cylinder (outer diameter 6 mm) and then was fixed during crystal structure refinements on sample data. TIPd_3H was measured in a vanadium cylinder (outer diameter 4 mm), the intermetallic phase in a sapphire crystal as sample holder (outer diameter 12 mm, inner diameter 6 mm), both during 20 minutes at $T = 298(2)$ K in air. More details to the sapphire container are given elsewhere [24]. For Rietveld refinements of the crystal structure on neutron powder data the following parameters were allowed to vary: the zero point of the 2θ scale, one scale, three peak width (Cagliotti formula. u , v and w), one mixing (η), two asymmetry parameters, beyond, for TIPd_3H four background parameters (polynomial), one lattice and three isotropic thermal displacement parameters, for TIPd_3 six background parameters (polynomial), two lattice, two positional and two isotropic thermal displacement parameters. The Rietveld plots are shown in Figures 1a and 1b, refined structure parameters are listed in Tables 1 and 2.

2.4. Thermal Analysis

Hydrogen absorption measurements were performed with a special gas pressure cell on a differential scanning calorimeter Q 1000 (TA instruments). 50-70 mg of the TIPd_3 samples were poured in an aluminium crucible which was closed with an aluminium lid and then placed inside the pressure cell. After flushing the chamber multiple times with hydrogen, the gas pressure was generally regulated at room temperature to around 1.5 bar and then the samples were heated up to 500°C or 320°C with a heating rate of 10°C per minute. The maximum temperature was held for 1 hour. After cooling to 40°C also with 10°C per minute two further cycles under the same conditions were recorded. After deflating hydrogen pressure the samples were characterized by XRPD.

3. Results and Discussion

3.1. Structure of TIPd_3

The obtained diffraction data show the pattern of a tetragonal unit cell with $a = 410.659(9)$ pm and $c = 1530.28(4)$ pm for the neutron data. The intensities match to those of the ZrAl_3 -type structure (space group $I4/mmm$, No.139; Figure 2a), which is a tetragonally distorted, ordered superstructure of the Cu structure type [30]. This tetragonal structure type was already proposed by Schubert et al. and Bhan et al. as the room temperature structure for TIPd_3 [33, 34]. The high temperature phase with TiAl_3 structure described by Schubert et al. and Bhan et al. [33, 34] was not observed during our experiments. The neutron diffraction pattern given in Figure 1a provide the first refined crystal structure for TIPd_3 from neutron data which are in agreement with structure data determined for the same sample by x-ray powder data (see Table 3). The lattice parameter reported by Schubert et al. $a = 411.7$ pm and $c = 1527.4$ pm [33] are concordantly to our sample synthesized from the elements with a reaction time of 60 hours (Table 3), but differ a bit for them with longer reaction times. However, the c/a ratio for all samples with ZrAl_3 structure is 0.93. Refinement of the free positional z parameters in the two Wyckoff positions $4e$ of the structure (Table 1) for the neutron data resulted in values close the idealized ones $z(\text{Ti}) = 0.125$ and $z(\text{Pd}_3) = 0.375$ [30], for both the deviation is not significant applying the 5σ criterion (Table 1) but the determined values are similar to those observed by Wannek for MgPd_3 owning the same structure type ($z(\text{Mg}) = 0.1242(10)$ and $z(\text{Pd}_3) = 0.3742(2)$) [22]. The palladium-palladium distances vary from $277.7(5)$ pm to $290.4(1)$ pm, the distances for palladium-thallium vary between $279.6(3)$ pm and $290.4(1)$ pm, also comparable to the distances known for MgPd_3 (ZrAl_3 type structure) [21, 22] as well as with InPd_3 (ZrAl_3 type structure) [30].

3.2. Structure of TIPd_3H

TIPd_3H was formed as product after reaction of TIPd_3 or the oxide phase TIPd_3O_4 in hydrogen gas at elevated temperatures (Table 3). From X-ray diffraction data TIPd_3H was found to crystallize in the cubic space group $Pm\bar{3}m$ (No.221) [Figure 2b]. The sublattice, which is built by metal atoms, forms a AuCu_3 type structure. From neutron data the hydrogen position (Table 2) was determined using difference Fourier analysis. For TIPd_3H the void is found to be occupied, which is in the centre of the unit cell ($\frac{1}{2} \frac{1}{2} \frac{1}{2}$) and surrounded by six palladium atoms. Refinement of the occupation factor resulted within the standard deviation in total occupation of this hydrogen position, for which reason the occupation parameter was fixed to the value 1. Beyond this, no significant occupation of the second remaining octahedral site on the edge centre ($\frac{1}{2} 0 0$) was found. In comparison to the intermetallic compound the neutron diffraction pattern of the hydride shown in Figure 1b exhibits a slightly enhanced, sloped background due to the incoherent scattering of ^1H . Nevertheless, because of the high quality of the presented data, Rietveld refinements yielded precise crystal structure parameters thus deuteration was not necessary. The difference between deuterides and hydrides was investigated recently by Henry et al. [40] and Ting et al. [41] and only small variation in structural parameters was observed in general.

The relative volume increase per formula unit $\Delta V/V_0$ is $3.9(1)\%$ for all completely transformed samples TIPd_3H (see Table 3) and $\Delta V/V_0 = 3.6$ or 3.7% for partially hydrogenated samples with AuCu_3 type metal atom sublattice. For the latter this accords to a TIPd_3H_x phase with x estimated to be about 0.9 assuming a linear relationship between x and $\Delta V/V_0$. This indicates a small homogeneity range with respect to the hydrogen content.

This cubic hydride phase will be called β -TIPd₃H in the following in order to distinguish it from a tetragonal hydride phase of TIPd₃ described below (3.3.).

The atomic arrangement of β -TIPd₃H corresponds to a completely filled cubic anti-perovskite type structure with a volume per formula unit about 4% higher compared to the intermetallic phase. Therewith, β -TIPd₃H which is stable in air under ambient conditions joins the class of ternary hydrides with perovskite structure. Many of them possess a cubic perovskite structure [42-47] but there are also some with cubic anti-perovskite structure: AlTi₃H [48], SnTi₃H [49], CeRh₃D_{0.84} [50], SnMn₃H [51], MnPd₃D_{0.7} [20], MgPd₃D_{0.7} [23] and InPd₃H_{-0.8} [31].

In the system thallium-palladium-hydrogen TIPd₃H is the first ternary hydride phase reported and in literature the structure of only one further thallium containing hydride was found [52], which is described as a Zintl Phase stabilized by hydrogen with the composition Na₁₅K₆Tl₁₈H. The hydrogen in this Zintl phase is enclosed in Tl octahedra with Tl-H distances of 232 pm. Compared to this, it is remarkable that hydrogen in the case of β -TIPd₃H prefers the voids with six palladium atoms as nearest neighbours. The palladium hydrogen distance of 203 pm is comparable to the Pd-D distances observed for pure PdD_{-0.7} (201 pm) [53] as well as for the palladium rich systems MnPd₃D_{0.67} (196 pm) [20] and for MgPd₃D_{0.67} (199 pm) [23]. Periodic XRD measurements showed the stability of the powdery hydride over 3 months in air under ambient conditions.

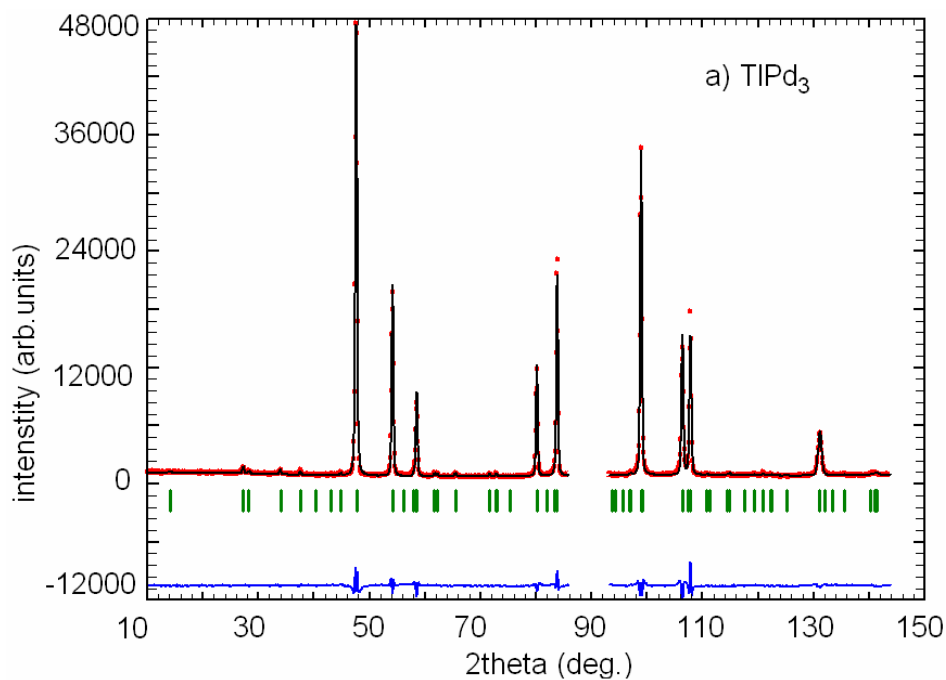
3.3. Formation and decomposition of TIPd₃H

Hydrogenation experiments with the intermetallic phase at room temperature up to 280 bar hydrogen pressure in an autoclave during 20 days showed no significant alteration in XRD pattern. After heating to 250 (\pm 10) °C under the same pressure for 24 hours a hydrogen uptake seen by a small rise of the cell parameter in the ZrAl₃-type phase was observed and the new phase with antiperovskite type structure (β -TIPd₃H) was built. This observation suggests not only hydrogen incorporation in the starting structure obtaining at least one phase, which will be called α -TIPd₃H_x below, but also that hydrogen uptake was not completed in the end of the experiment.

Whereas, TIPd₃ and TIPd₃O₄ heated at 730°C for 12 hours in 1bar hydrogen atmosphere were found to build the hydride β -TIPd₃H as single phase (Table 3). When 7.5% hydrogen in argon is used as reaction gas the product is a mixture of α -TIPd₃H_x with an expanded unit cell in respect to TIPd₃ (0.6 % respectively 0.8% per formula unit) and β -TIPd₃H, which indicates that the hydrogen partial pressure was not high enough in these cases to hydrogenate the samples fully in this time. Furthermore one of the 5-phase-mixtures (see Section 2.1.) was likewise heated in hydrogen/argon atmosphere and ended just like the educts TIPd₃ and TIPd₃O₄ in a mixture of α -TIPd₃H_x and β -TIPd₃H (Table 3). Assuming that the observed lattice expansion is solo caused by hydrogen uptake and the two are related linearly, the α -phase is estimated to be TIPd₃H_{-0.2}, since $\Delta V/V_0 \approx 3.9$ % is equivalent to TIPd₃H. Furthermore, heating anew a mixture of α -TIPd₃H_x and β -TIPd₃H at 730°C for 12 hours in hydrogen/argon atmosphere resulted in no significant changes in phase fractions. Out of this can be inferred that the temperature treatment can be moderate but it is very important to apply a hydrogen partial pressure high enough to complete hydrogenation forming β -TIPd₃H.

The formation pathway of β -TIPd₃H_x with as starting material could be topotactical, in case of β -TIPd₃H_x the TIPd₃ substructure is a AuCu₃ type structure (Figure 2b) and in case of TIPd₃O₄ it is 2 x 2 x 2 superstructure of the AuCu₃ type structure (Figure 2c). This fact could be the explanation that the amount of β -TIPd₃H_x is higher for TIPd₃O₄ as for both other starting materials under same reaction conditions. However it seems more likely that the smaller particle size of the oxide as compared to the intermetallic phase causes the above mentioned enhanced reactivity. Further hydrogenation experiments some of them carried out in the gas pressure cell of the DSC (Section 2.4.) demonstrated that temperatures of 500°C and also of 320°C for even clearly less than 12 hours suffice to observe the full hydrogenation of TIPd₃ in hydrogen gas atmosphere around 1bar. DSC measurements (Figure 3) showed an exothermic reaction during hydrogen absorption over a wide temperature range. The broad exothermic signal has two maxima, one around 280°C and a second in the region of 370°C. These detected maxima could be a hint of a stepwise reaction during hydrogen incorporation as already assumed. Nevertheless DSC measurements up to only 320°C and held there for 1 hour resulted in a complete hydrogenated, cubic anti-perovskite type structured sample. Since the cooling branches show no signal the hydrogen uptake is not reversible under these conditions. The stability of the hydride at ambient conditions in air over months also was observed (Section 3.2.).

In order to study the thermal stability of TIPd₃H_x its behaviour under dynamic vacuum and elevated temperature was investigated. Evacuation of the pure β -TIPd₃H samples in the dynamic vacuum ($p \approx 10^{-1}$ mbar) over 16 hours at 120°C -130°C showed a small volume per formula decrease ($\leq 0.2\%$) only, whereas upon reheating to 230°C under the same conditions the hydride released hydrogen to rebuild again TIPd₃ in the known tetragonal structure (Figure 2a). A 1:1 α -TIPd₃H_x and β -TIPd₃H sample obtained in an atmosphere of 7.5% hydrogen in argon (see above) was investigated using the same temperature treatment. The α -TIPd₃H_x phase showed at 120°C -130°C as well as at 230°C a volume decrease of $\sim 0.4\%$ per formula unit. The β -TIPd₃H phase showed similar behaviour as pure β -TIPd₃H samples. In the end this mixed sample also resulted in TIPd₃ (ZrAl₃-type) as single phase (Table 3).



33
34
35
36
37
38
39

Figure 1a. ((Rietveld refinement on neutron powder diffraction data of TIPd_3 (D20 at ILL (Grenoble, France), $\lambda = 186.893(2)\text{pm}$, $T=298(2)\text{K}$). Observed (dots), calculated (solid line) and difference (observed-calculated, bottom) neutron powder diffraction patterns. Bragg peak positions of TIPd_3 in the ZrAl_3 type structure. Excluded region $86^\circ \leq 2\theta \leq 93^\circ$ for Rietveld refinement was chosen because of a contribution to the diffraction pattern caused by the sapphire sample holder))

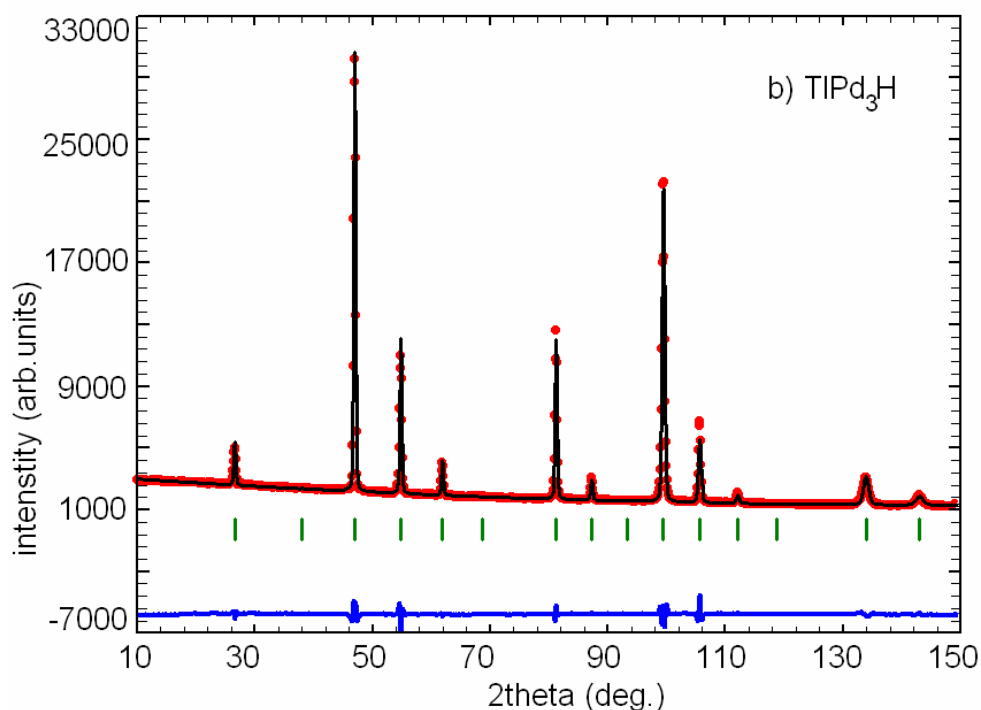


Figure 1b. ((Rietveld refinement on neutron powder diffraction data of TiPd_3H (D20 at ILL (Grenoble, France), $\lambda = 186.893(2)\text{pm}$, $T=298(2)\text{K}$). Observed (dots), calculated (solid line) and difference (observed-calculated, bottom) neutron powder diffraction patterns. Bragg peak positions of TiPd_3H in the anti-perovskite type structure))

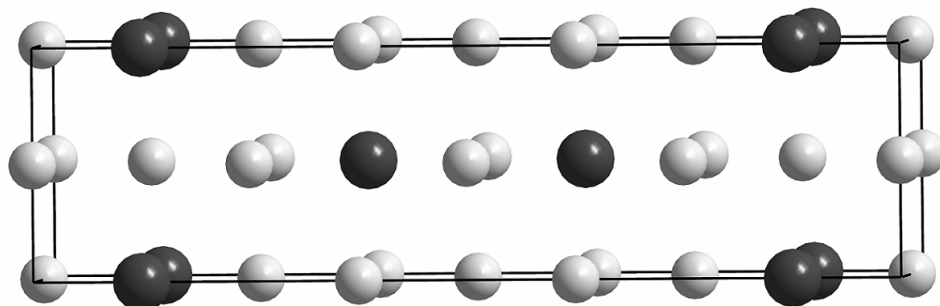


Figure 2a. ((Crystal structure of TiPd_3 (ZrAl_3 type), dark grey spheres represent thallium and bright grey spheres palladium))

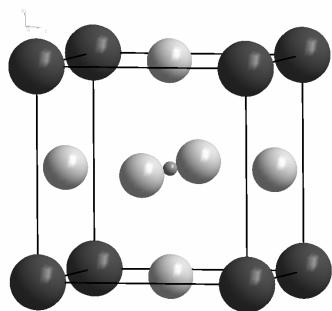


Figure 2b. ((Crystal structure of TiPd_3H (cubic anti-perovskite type), dark grey spheres represent thallium, bright grey spheres palladium and small middle grey spheres hydrogen))

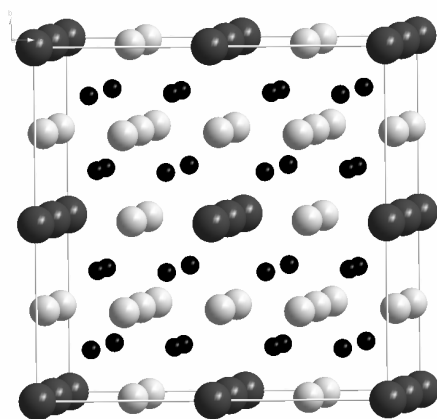


Figure 2c. ((Crystal structure of TlPd_3O_4 (Tl and Pd form a $2 \times 2 \times 2$ superstructure of the AuCu_3 structure with oxygen located in one half of the tetrahedral sites) according to Ref. [36], dark grey spheres represent thallium and bright grey spheres palladium and small black spheres oxygen))

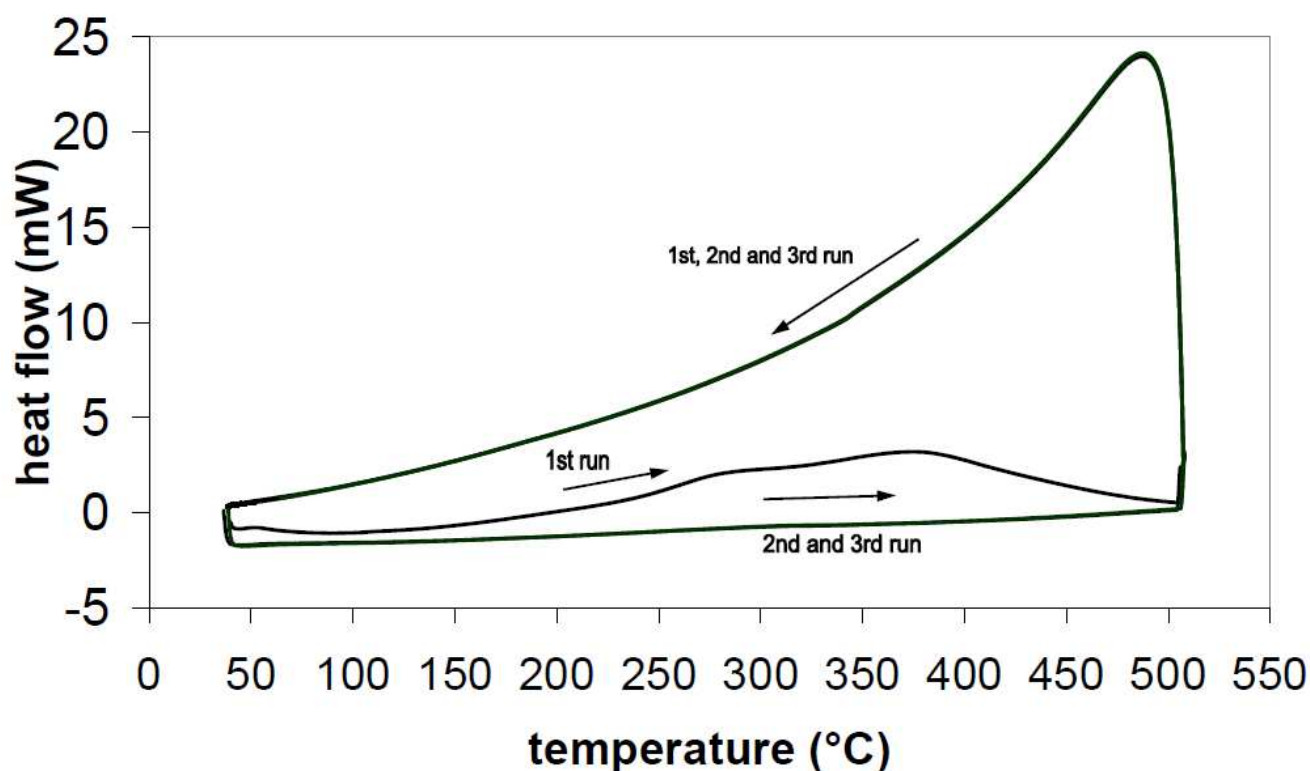


Figure 3. ((DSC curves of TlPd_3 under 1.5 bar H_2 , heating rate $10^\circ\text{C}/\text{min}$, exothermic signal up))

Table 1. ((Crystal structure parameters and atomic distances of TlPd_3 at room temperature from neutron powder diffraction data space group $I4/mmm$ (No.139): $a = 410.659(9)$ pm, $c = 1530.28(4)$ pm, $V = 258.068(11) \times 10^6$ pm³.)

Atom	Site	x	y	z	$B_{\text{iso}}/10^4$ pm
Tl	4e	0	0	0.1240(3)	0.67(5)
Pd1	4c	0	1/2	0	0.67(4)
Pd2	4d	0	1/2	1/4	$B_{\text{iso}}(\text{Pd1})$
Pd3	4e	0	0	0.3778(5)	$B_{\text{iso}}(\text{Pd1})$
Pd1-Pd1: 290.4(1) pm				Pd1-Tl: 279.6(3) pm	
Pd1-Pd3: 277.7(5) pm				Pd2-Tl: 281.7(3) pm	
Pd2-Pd3: 283.6(3) pm				Pd3-Tl: 290.4(1) pm	

$R_p = 0.054$, $R_{\text{wp}} = 0.072$, $R'_p = 0.122$, $R'_{\text{wp}} = 0.118$, $R_{\text{Bragg}} = 0.031$. Definition of R factors: $R_p = \sum |y_i(\text{obs}) - y_i(\text{calc})| / \sum y_i(\text{obs})$; $R_{\text{wp}} = [\sum w_i (y_i(\text{obs}) - y_i(\text{calc}))^2]^{1/2}$; R'_p and R'_{wp} are calculated as above but using background corrected counts; $R_{\text{Bragg}} = \sum I_B('obs') - I_B(\text{calc}) / \sum I_B('obs')$. Form of the temperature factor: $\exp[-B_{\text{iso}}(\sin\theta/\lambda)^2]$.

Table 2. ((Crystal structure parameters and atomic distances of TlPd_3H at room temperature from neutron powder diffraction data space group $Pm\bar{3}m$ (No.221): $a = 406.313(1)$ pm, $V = 67.078(3) \times 10^6$ pm³.)

Atom	Site	x	y	z	$B_{\text{iso}}/10^4$ pm
Tl	1a	0	0	0	0.47(5)
Pd	3c	1/2	1/2	0	0.50(3)
H	1b	1/2	1/2	1/2	2.6(2)
Pd-H: 203.2(1) pm				Pd-Tl: 287.(1) pm	

$R_p = 0.021$, $R_{\text{wp}} = 0.033$, $R'_p = 0.143$, $R'_{\text{wp}} = 0.103$, $R_{\text{Bragg}} = 0.045$. Definition of R_p , R_{wp} , R'_p , R'_{wp} , R_{Bragg} and form of the temperature factor see Table 1

Table 3. ((Overview of the lattice parameters of $TiPd_3$ and its hydrides determined by x-ray diffraction (labelled with * means determined by neutron diffraction).))

starting material	T, time	P (gas)	Mass %	Product phases	Metal sub-lattice	a [pm]	c [pm]	V (f.u. $TiPd_3$) [10^6 pm^3]	$\Delta V/V_0$ [%]
elements Ti, Pd	600°C 160 h	evacuated silica tube	100	$TiPd_3$	ZrAl ₃	410.403(2)	1530.56(1)	64.448(3)	- 0.1
	*	*	*	*	*	410.659(9)	1530.28(4)	64.515(1)	$0 = V_0$
	600°C 60 h	evacuated silica tube	100	$TiPd_3$	ZrAl ₃	411.400(3)	1526.89(2)	64.607(4)	+ 0.1
$TiPd_3$	730°C 12 h	H ₂ , 1bar	100	β - $TiPd_3H$	AuCu ₃	406.104(4)		66.975(1)	+ 3.8
	320°C 1 h	H ₂ , DSC 1.5bar	100	β - $TiPd_3H$	AuCu ₃	406.195(5)		67.020(1)	+ 3.9
	500°C 1 h	H ₂ , DSC 1.5bar	100	β - $TiPd_3H$	AuCu ₃	406.252(2)		67.048(1)	+ 3.9
	500°C 10 h	H ₂ , 1bar	100	β - $TiPd_3H$	AuCu ₃	406.272(4)		67.058(1)	+ 3.9
	*	*	*	*	*	406.313(1)		67.078(3)	+ 3.9
	730°C 12 h	7.5% H ₂ /Ar 1bar	86 14	α - $TiPd_3H$ β - $TiPd_3H$	ZrAl ₃ AuCu ₃	411.133(5) 405.84(1)	1536.27(3)	64.919(7) 66.844(3)	+ 0.6 + 3.6
$TiPd_3O_4$	730°C 12 h	N ₂ , 1bar	100	$TiPd_3$	ZrAl ₃	410.454(3)	1531.05(1)	64.485(4)	- 0.1
	730°C 12 h	7.5% H ₂ /Ar 1bar	18 82	α - $TiPd_3H$ β - $TiPd_3H$	ZrAl ₃ AuCu ₃	410.34(3) 406.077(6)	1544.5(2)	65.018(4) 66.962(2)	+ 0.8 + 3.8
	730°C 12 h	H ₂ , 1bar	100	β - $TiPd_3H$	AuCu ₃	406.092(2)		66.969(1)	+ 3.8
5 phase mixture	730°C 12 h	7.5% H ₂ /Ar 1bar	64 36	α - $TiPd_3H$ β - $TiPd_3H$	ZrAl ₃ AuCu ₃	411.351(8) 405.980(6)	1535.18(4)	64.943(1) 66.914(2)	+ 0.7 + 3.7
α - $TiPd_3H$, β - $TiPd_3H$	120- 130°C 16 h	vacuum	55 45	α - $TiPd_3H$ β - $TiPd_3H$	ZrAl ₃ AuCu ₃	410.695(6) 405.804(6)	1534.94(3)	64.725(8) 66.827(2)	+ 0.3 + 3.6
	230°C 16 h	vacuum	100	$TiPd_3$	ZrAl ₃	410.640(2)	1529.15(2)	64.463(3)	- 0.1
β - $TiPd_3H$	120- 130°C 16h	vacuum	100	β - $TiPd_3H$	AuCu ₃	406.033(3)		66.939(1)	+ 3.6
	230°C 16 h	vacuum	100	$TiPd_3$	ZrAl ₃	410.635(3)	1529.23(2)	64.465(4)	- 0.1

4. Conclusion

Synthesis of $TiPd_3$ from the elements or $TiPd_3O_4$ as starting materials was investigated. The ZrAl₃ type structure proposed in literature for the intermetallic compound was confirmed. First structure refinements for $TiPd_3$ were performed and resulted in structural parameters very similar to those of other MPd_3 phases (M = Mg and In). Formation of $TiPd_3H_x$ was achieved by reduction of the oxide phase $TiPd_3O_4$ in hydrogen gas atmosphere. The hydrogenation of $TiPd_3$ also resulting in $TiPd_3H_x$ was studied by NPD, XRPD and in situ DSC. For high pressure of 280 bar no significant hydrogen absorption at room temperature was found, but at 250(±10)°C. At around 1 bar hydrogen gas pressure, formation of the previously unknown

hydride β -TlPd₃H (cubic anti-perovskite type structure, space group $Pm\bar{3}m$, $a = 406.313(1)$ pm, $\Delta V/V_0 = 3.9\%$) was observed at temperatures of 320°C up to 730°C. Depending mostly on temperature the reaction progress was followed by ex and in situ methods showing the existence of α -TlPd₃H_x (tetragonal ZrAl₃-type like metal atom lattice) and β -TlPd₃H_x (cubic AuCu₃-type like metal atom lattice) who are structurally related. TlPd₃ as well as α -TlPd₃H_x differ from β -TlPd₃H_x in having anti-phase boundaries $\frac{1}{2}$ [110] which are removed during hydrogen uptake progress. Dehydrogenation experiments of the TlPd₃H_x phases under dynamic vacuum over 16 hours showed a small hydrogen release at around 125°C and total dehydrogenation at 230°C.

5. Acknowledgments

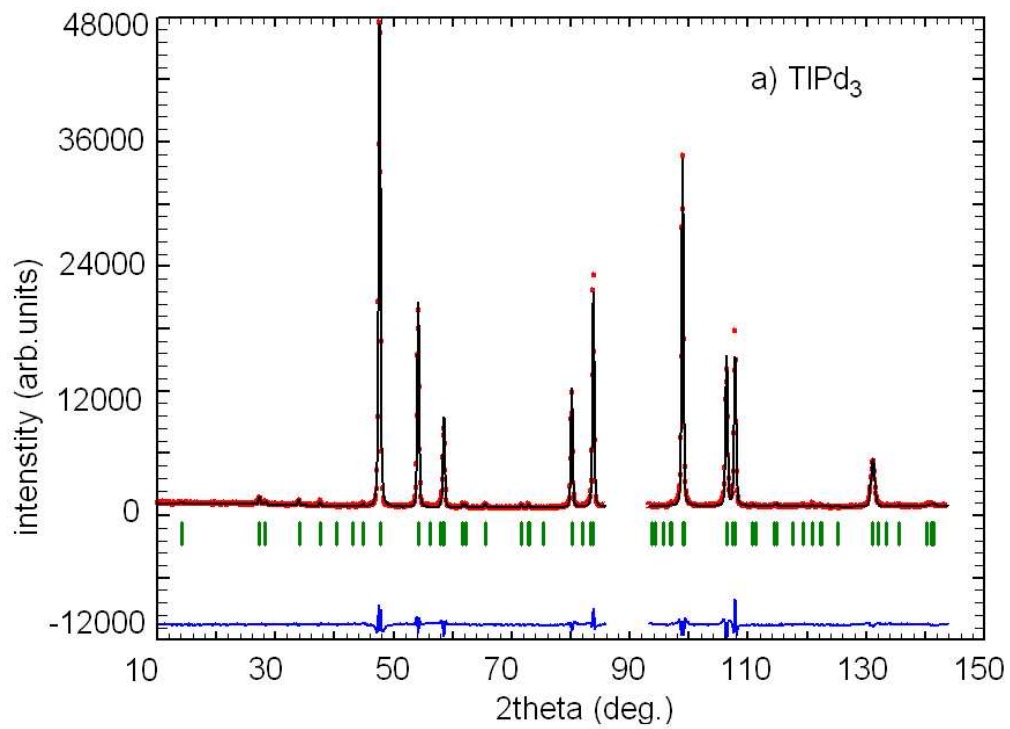
This work has been supported by the Deutsche Forschungsgemeinschaft (grant Ko1803/2), the Institut Laue Langevin within the long term proposal LTP-5A-1 and by Saarland University (PhD scholarship). We thank Thomas Hansen (ILL) for his support with the neutron diffraction experiments as well as Silvia Beetz and Hermann Recktenwald for technical assistance with the construction of the fittings for the gas pressure cell.

- [1] T. B. Flanagan, F. A. Lewis, *Z. Phys. Chem. Neue Folge* **1961**, 27, 104-111.
- [2] F.A. Lewis, *Platinum Met. Rev.* **1982**, 26, 20-27, 70-78 and 121-128.
- [3] L. Schlapbach, *Hydrogen in Intermetallic Compounds I*, Springer-Verlag, **1988**, 1-10.
- [4] G. Wiesinger, G. Hilscher, *Handbook of Magnetic Materials* (K. H. J. Buschow, Ed.), Elsevier, Amsterdam, **2008**, Vol. 17, 293-456.
- [5] A. R. Miedema, K. H. J. Buschow, H. H. Van Mal, *J. Less-Common Met.* **1976**, 49, 463-472.
- [6] S. Miraglia, D. Fruchart, E. K. Hlil, S. S. M. Tavares, D. Dos Santos, *J. Alloys Compd.* **2001**, 317-318, 77-82.
- [7] R. Nakayama, T. Takeshita, *J. Appl. Phys.* **1993**, 74, 2719-2724.
- [8] P. Önnnerud, Y. Andersson, R. Tellgren, P. Norblad, F. Bourée, G. André, *Solid State Commun.* **1997**, 101, 433-437.
- [9] H. Vehoff, in H. Wipf (Ed.), *Hydrogen Materials III, Top. Appl. Phys.* **1997**, 73, 215-278.
- [10] E. Akiba, *Current Opinion in Solid State Mater. Sci.* **1999**, 4, 267-272.
- [11] J. L. Soubeyroux, D. Fruchart, A. S. Biris, *Phys. B* **1998**, 241-243, 341-343.
- [12] J.J. Reilly, R. H. Wiswall, *Inorg. Chem.* **1967**, 6, 2220-2223 and **1968**, 7, 2254-2256.
- [13] R. Balasubramaniam, *Scr. Metall. Mater.* **1994**, 30(7), 875-880.
- [14] P. Kumar, M. Hareesh, R. Balasubramaniam, *J. Alloys Compd.* **1995**, 217, 151-156.
- [15] T. B. Flanagan, Y. Sakamoto, *Platinum Met. Rev.* **1993**, 37, 26-37.
- [16] T. B. Flanagan, H. Noh, J. Clewley, *Pol. J. Chem.* **1997**, 71, 1725-1734.
- [17] T. B. Flanagan, S. Luo, *J. Phys. Chem. B* **2006**, 110, 8080-8086.
- [18] R. Tellgren, Y. Andersson, I. Goncharenko, G. André, F. Bourée, I. Mirebeau, *J. Solid State Chem.* 2001, 161, 93-96.
- [19] K. J. Baba, Y. Niki, Y. Sakamoto, *J. Less-Common Met.* **1991**, 172-174, 246-253.
- [20] J. P. Ahlzen, Y. Andersson, R. Tellgren, D. Rodic, *Z. Phys. Chem. Neue Folge* **1989**, 163, 213-218.
- [21] C. Wannek, B. Harbrecht, *J. Solid State Chem.* **2001**, 159, 113-120.
- [22] C. Wannek, *Dissertation*, Univ. Marburg **2001**.
- [23] H. Kohlmann, G. Renaudin, K. Yvon, C. Wannek, B. Harbrecht, *J. Solid State Chem.* **2005**, 178, 1292-1300.
- [24] H. Kohlmann, N. Kurtzemann, R. Wehrich, T. Hansen, *Z. Anorg. Allg. Chem.* **2009**, 635, 2399-2405.
- [25] C. Wannek, B. Harbrecht, *Z. Anorg. Allg. Chem.* **2007**, 633, 1397-1402.
- [26] K. Schubert, H. L. Lukas, H.-G. Meißner, S. Bhan, *Z. Metallkde.* **1959**, 50, 534-540.
- [27] S. Bhan, K. Schubert, *J. Less-Common Met.* **1969**, 17, 73-90.
- [28] C. Wannek, B. Harbrecht, *Z. Anorg. Allg. Chem.* **2000**, 626, 1540-1544.
- [29] H. Kohlmann, C. Ritter, *Z. Naturforsch. B* **2007**, 62, 929-934.
- [30] H. Kohlmann, C. Ritter, *Z. Anorg. Allg. Chem.* **2009**, 635, 1573-1579.
- [31] H. Kohlmann, *J. Solid State Chem.* **2010**, 183, 367-372.
- [32] H. H. Stadelmaier, W. K. Hardy, *Z. Metallkde.* **1961**, 52, 391-396.
- [33] K. Schubert, S. Bhan, T. K. Biswas, K. Frank, P. K. Panday, *Naturwissenschaften* **1968**, 55, 542-543.
- [34] S. Bhan, T. Gödecke, P. K. Panday, K. Schubert, *J. Less-Common Met.* **1968**, 16, 415-425.
- [35] H. Nowotny, K. Schubert, U. Dettinger, *Z. Metallkde.* **1946**, 37, 137-145.
- [36] C. Zöllner, G. Thiele, M. Müllner, *Z. Anorg. Allg. Chem.* **1978**, 443, 11-18.
- [37] M. Müllner, G. Thiele, C. Zöllner, *Z. Anorg. Allg. Chem.* **1978**, 443, 19-22.

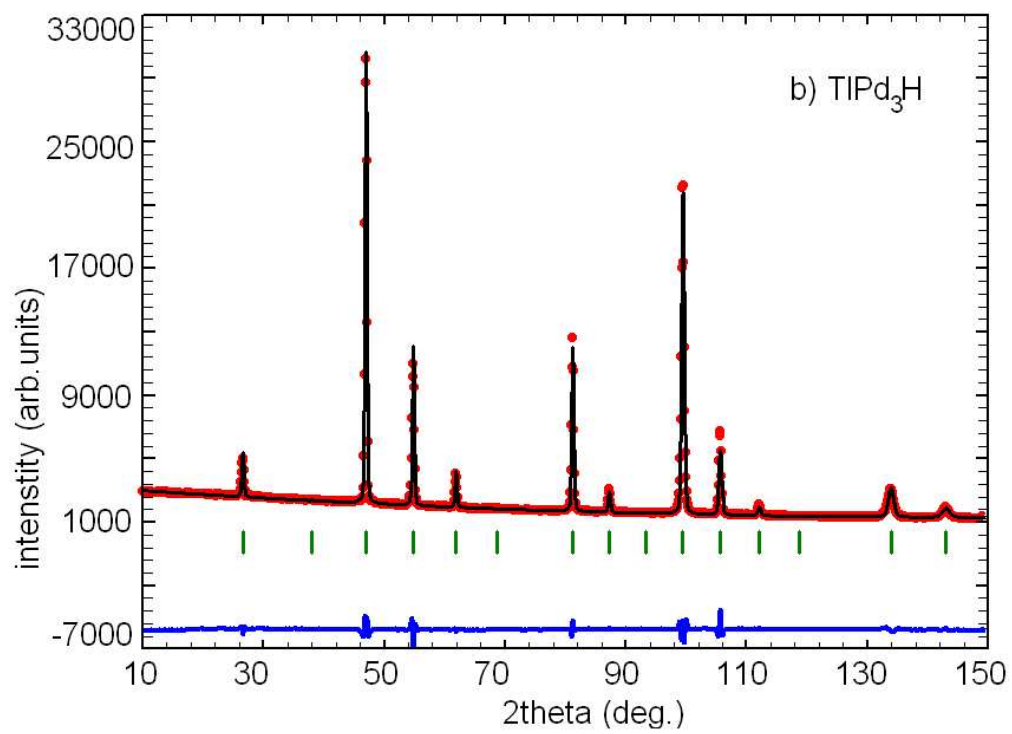
- 1
2 [38] J. Rodriguez-Carvajal, FullProf.2k, Version 4.50, Jan2009-ILL JCR, **2009**.
3 [39] T. C. Hansen, P. F. Henry, H. E. Fischer, J. Torresgrossa, P. Convert, *Meas. Sci. Technol.* **2008**, *19*, 034001.
4 [40] P. F. Henry, M. T. Weller, C. C. Wilson, *Chem. Commun. (Cambridge, U. K.)* **2008**, 1557-1559.
5 [41] V. P. Ting, P. F. Henry, C. C. Wilson, H. Kohlmann, M. T. Weller, *Phys. Chem. Chem. Phys.* **2010**, in press.
6 [42] C. E. Messer, J. Eastman, R. G. Mers, A. Maeland, *Inorg. Chem.* **1964**, *3*, 776-778.
7 [43] W. Bronger, K. Jansen, P. Müller, *J. Less-Common Met.* **1990**, *161*, 299-302.
8 [44] H. Kohlmann, K. Yvon, *J. Alloys Compds.* **2000**, *299*, L16.
9 [45] H. Kohlmann, H. E. Fischer, K. Yvon, *Inorg. Chem.* **2001**, *40*, 2608-2613.
10 [46] K. Yvon, H. Kohlmann, B. Bertheville, *Chimia* **2001**, *55*, 505-509.
11 [47] K. Yvon, B. Bertheville, *J. Alloys Compds.* **2006**, *425*, 101-108.
12 [48] D. S. Schwarz, W. B. Yelon, R. R. Berliner, R. J. Lederich, S. M. L. Sastry, *Acta Metall. Mater.* **1991**, *39*, 2799.
13 [49] M. Vennström, A. Grechnev, O. Eriksson, Y. Andersson, *J. Alloys Compds.* **2004**, *364*, 127-131.
14 [50] H. Kohlmann, F. Müller, K. Stöwe, A. Zalga, H. P. Beck, *Z. Anorg. Allg. Chem.* **2009**, *635*, 1407-1411.
15 [51] G. Grosse, F. E. Wagner, V. E. Antonov, T. E. Antonova, *J. Alloys Compds.* **1997**, *253-254*, 339-342.
16 [52] Z.-C. Dong, J. D. Corbett, *Inorg. Chem.* **1995**, *34*, 5709-10.
17 [53] J. E. Schirber, B. Morosin, *Phys. Rev. B: Condens. Matter* **1975**, *12*, 117-118.

23 Received: ((will be filled in by the editorial staff))
24 Published online: ((will be filled in by the editorial staff))
25
26
27
28
29
30
31
32
33
34
35
36
37
38
39
40
41
42
43
44
45
46
47
48
49
50
51
52
53
54
55
56
57
58
59
60

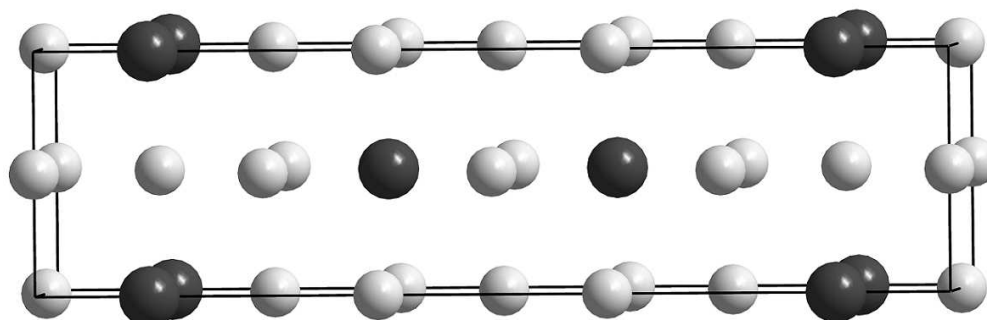
1
2
3
4
5
6
7
8
9
10
11
12
13
14
15
16
17
18
19
20
21
22
23
24
25
26
27
28
29
30
31
32
33
34
35
36
37
38
39
40
41
42
43
44
45
46
47
48
49
50
51
52
53
54
55
56
57
58
59
60



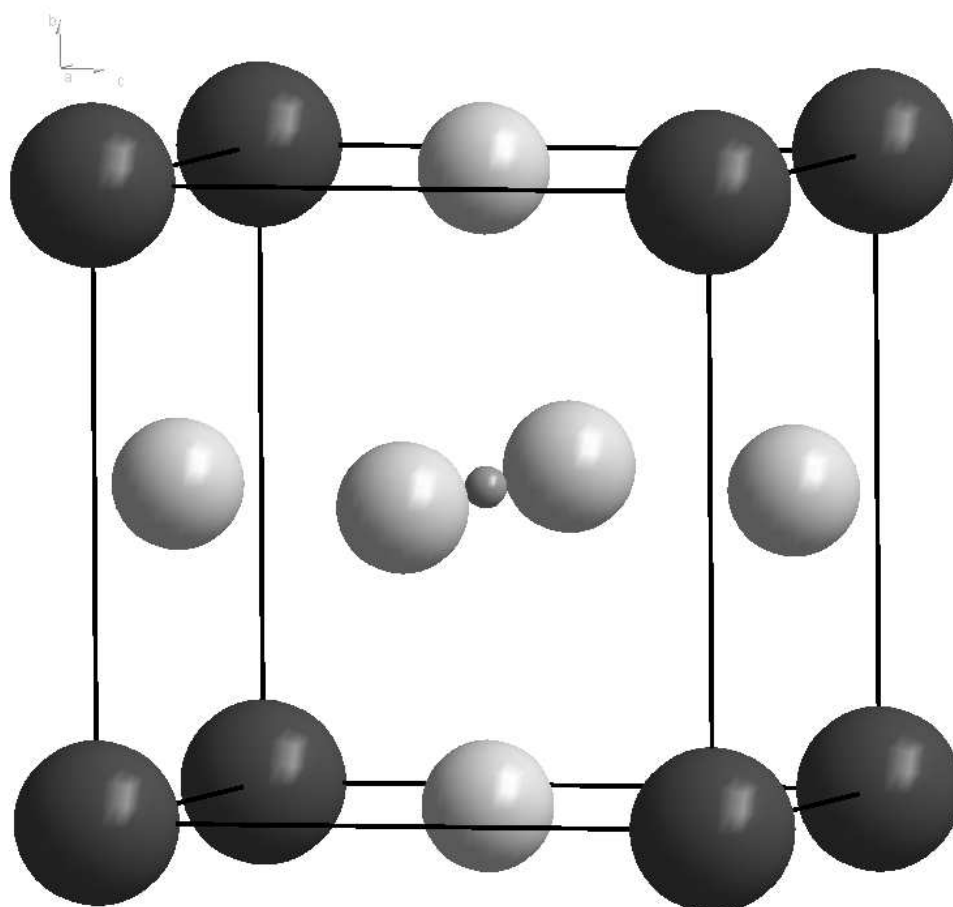
228x165mm (96 x 96 DPI)



224x167mm (96 x 96 DPI)

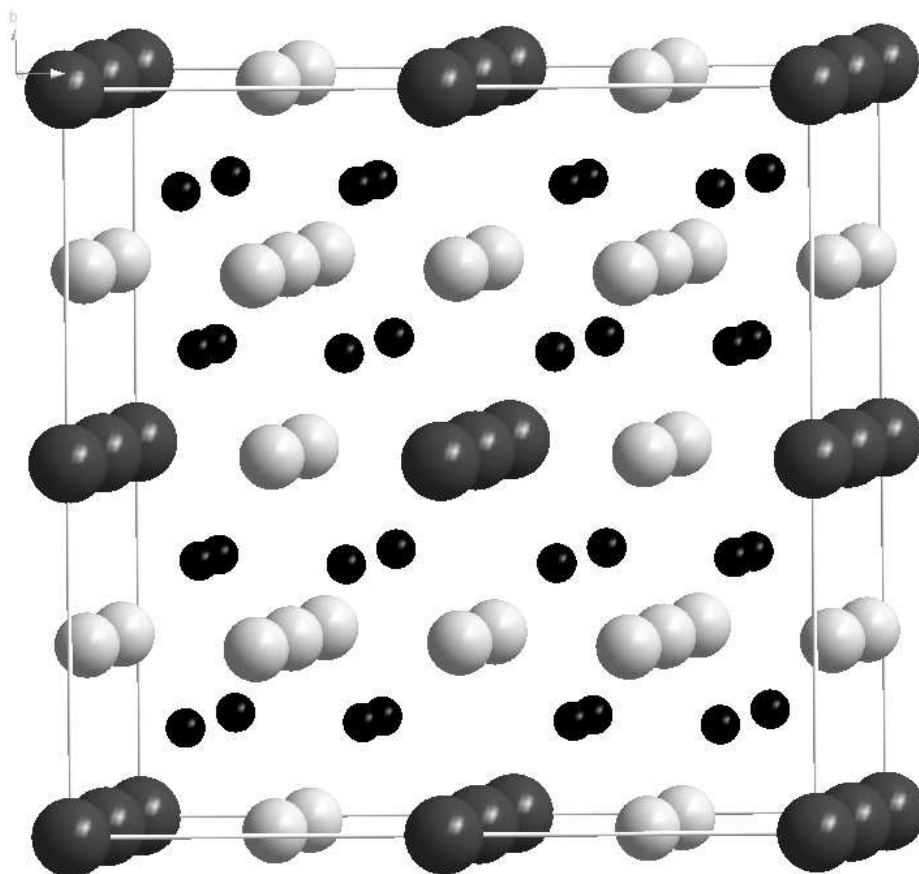


311x104mm (96 x 96 DPI)



((Crystal structure of TIPd₃H (cubic anti-perovskite type), dark grey spheres represent thallium, bright grey spheres palladium and small middle grey spheres hydrogen))
203x195mm (96 x 96 DPI)

1
2
3
4
5
6
7
8
9
10
11
12
13
14
15
16
17
18
19
20
21
22
23
24
25
26
27
28
29
30
31
32
33
34
35
36
37
38
39
40
41
42
43
44
45
46
47
48
49
50
51
52
53
54
55
56
57
58
59
60



203x195mm (96 x 96 DPI)

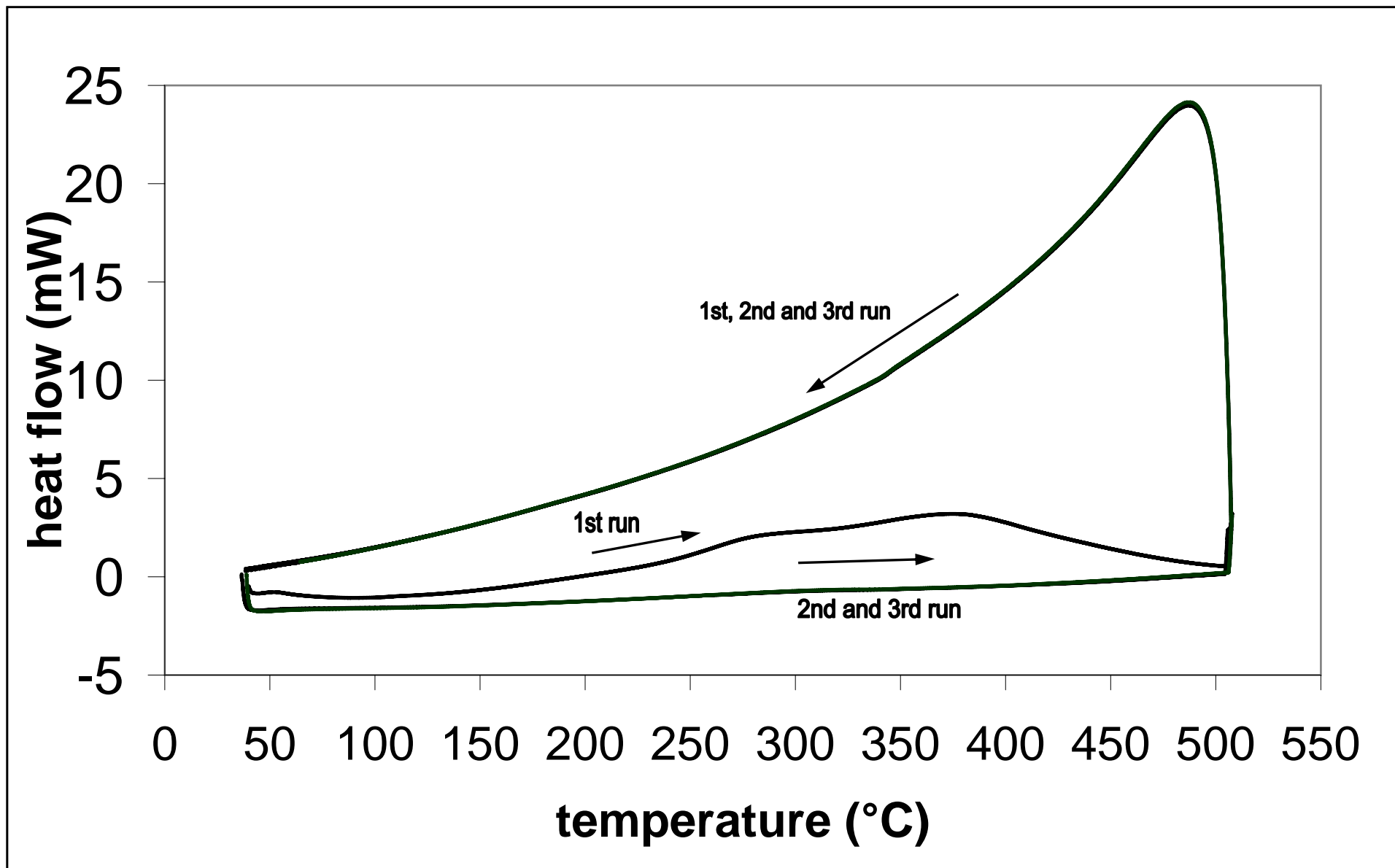


Table 1. ((Crystal structure parameters and atomic distances of TlPd_3 at room temperature from neutron powder diffraction data space group $I4/mmm$ (No.139): $a = 410.659(9)$ pm, $c = 1530.28(4)$ pm, $V = 258.068(11) \cdot 10^6$ pm³.)

Atom	Site	x	y	z	$B_{\text{iso}} / 10^4$ pm
Tl	4e	0	0	0.1240(3)	0.67(5)
Pd1	4c	0	½	0	0.67(4)
Pd2	4d	0	½	¼	$B_{\text{iso}}(\text{Pd1})$
Pd3	4e	0	0	0.3778(5)	$B_{\text{iso}}(\text{Pd1})$
Pd1-Pd1: 290.4(1) pm		Pd1-Tl: 279.6(3) pm			
Pd1-Pd3: 277.7(5) pm		Pd2-Tl: 281.7(3) pm			
Pd2-Pd3: 283.6(3) pm		Pd3-Tl: 290.4(1) pm			

$R_p = 0.054$, $R_{\text{wp}} = 0.072$, $R'_p = 0.122$, $R'_{\text{wp}} = 0.118$, $R_{\text{Bragg}} = 0.031$ Definition of R factors: $R_p = \sum |y_i(\text{obs}) - y_i(\text{calc})| / \sum y_i(\text{obs})$; $R_{\text{wp}} = [\sum w_i (y_i(\text{obs}) - y_i(\text{calc}))^2]^{1/2}$; R'_p and R'_{wp} are calculated as above but using background corrected counts; $R_{\text{Bragg}} = \sum I_{\text{B}}('obs') - I_{\text{B}}(\text{calc}) / \sum I_{\text{B}}('obs')$. Form of the temperature factor: $\exp [-B_{\text{iso}}(\sin\theta/\lambda)^2]$.

Table 2. ((Crystal structure parameters and atomic distances of TiPd_3H at room temperature from neutron powder diffraction data space group $Pm-3m$ (No.221): $a = 406.313(1)$ pm, $V = 67.078(3) \cdot 10^6$ pm³.)

Atom	Site	x	y	z	$B_{\text{iso}}/10^4$ pm
Ti	1a	0	0	0	0.47(5)
Pd	3c	½	½	0	0.50(3)
H	1b	½	½	½	2.6(2)

Pd-H: 203.2(1) pm Pd-Ti: 287.(1) pm

$R_p = 0.021$, $R_{\text{wp}} = 0.033$, $R'_p = 0.143$, $R'_{\text{wp}} = 0.103$, $R_{\text{Bragg}} = 0.045$. Definition of R_p , R_{wp} , R'_p , R'_{wp} , R_{Bragg} and form of the temperature factor see Table 1

starting material	T, time	P (gas)	Mass %	Product phases	Metal sub-lattice	a [pm]	c [pm]	V (f.u. TIPd ₃) [10 ⁶ pm ³]	ΔV/V ₀ [%]
elements Tl, Pd	600°C 160 h	evacuated silica tube	100	<i>TlPd₃</i>	ZrAl ₃	410.403(2)	1530.56(1)	64.448(3)	- 0.1
	*	*	*	*	*	410.659(9)	1530.28(4)	64.515(1)	0 = V₀
	600°C 60 h	evacuated silica tube	100	<i>TlPd₃</i>	ZrAl ₃	411.400(3)	1526.89(2)	64.607(4)	+ 0.1
TlPd₃	730°C 12 h	H ₂ , 1bar	100	<i>β-TlPd₃H</i>	AuCu ₃	406.104(4)		66.975(1)	+ 3.8
	320°C 1 h	H ₂ , DSC 1.5bar	100	<i>β-TlPd₃H</i>	AuCu ₃	406.195(5)		67.020(1)	+ 3.9
	500°C 1 h	H ₂ , DSC 1.5bar	100	<i>β-TlPd₃H</i>	AuCu ₃	406.252(2)		67.048(1)	+ 3.9
	500°C 10 h	H ₂ , 1bar	100	<i>β-TlPd₃H</i>	AuCu ₃	406.272(4)		67.058(1)	+ 3.9
	*	*	*	*	*	406.313(1)		67.078(3)	+ 3.9
	730°C 12 h	7.5% H ₂ /Ar 1bar	86 14	<i>α-TlPd₃H</i> <i>β-TlPd₃H</i>	ZrAl ₃ AuCu ₃	411.133(5) 405.84(1)	1536.27(3)	64.919(7) 66.844(3)	+ 0.6 + 3.6
TlPd₃O₄	730°C 12 h	N ₂ , 1bar	100	<i>TlPd₃</i>	ZrAl ₃	410.454(3)	1531.05(1)	64.485(4)	- 0.1
	730°C 12 h	7.5% H ₂ /Ar 1bar	18 82	<i>α-TlPd₃H</i> <i>β-TlPd₃H</i>	ZrAl ₃ AuCu ₃	410.34(3) 406.077(6)	1544.5(2)	65.018(4) 66.962(2)	+ 0.8 + 3.8
	730°C 12 h	H ₂ , 1bar	100	<i>β-TlPd₃H</i>	AuCu ₃	406.092(2)		66.969(1)	+ 3.8
5 phase mixture	730°C 12 h	7.5% H ₂ /Ar 1bar	64 36	<i>α-TlPd₃H</i> <i>β-TlPd₃H</i>	ZrAl ₃ AuCu ₃	411.351(8) 405.980(6)	1535.18(4)	64.943(1) 66.914(2)	+ 0.7 + 3.7
α-TlPd₃H, β-TlPd₃H	120- 130°C 16 h	vacuum	55 45	<i>α-TlPd₃H</i> <i>β-TlPd₃H</i>	ZrAl ₃ AuCu ₃	410.695(6) 405.804(6)	1534.94(3)	64.725(8) 66.827(2)	+ 0.3 + 3.6
	230°C 16 h	vacuum	100	<i>TlPd₃</i>	ZrAl ₃	410.640(2)	1529.15(2)	64.463(3)	- 0.1
β-TlPd₃H	120- 130°C 16h	vacuum	100	<i>β-TlPd₃H</i>	AuCu ₃	406.033(3)		66.939(1)	+ 3.6
	230°C 16 h	vacuum	100	<i>TlPd₃</i>	ZrAl ₃	410.635(3)	1529.23(2)	64.465(4)	- 0.1